CHIN. PHYS. LETT. Vol. 27, No. 8 (2010) 087303

Co-occurrence of Dominant Direct and Indirect Transitions in Low Temperature Sputtered Indium Tin Oxide Thin Films on Polymers *

YIN Xue-Song(殷学松), TANG Wu(唐武)**, WENG Xiao-Long(翁小龙), DENG Long-Jiang(邓龙江)

State Key Laboratory of Electronic Thin Films and Integrated Devices, University of Electronic Science and Technology of China, Chengdu 610054

(Received 29 October 2009)

Indium tin oxide (ITO) layers are prepared on polymethylmethacrylate and polyethylene terephthalate by rf-magnetron sputtering at room temperature. Their 3D-AFM images and visible transmittance spectra are contrastively characterized and studied. An interesting morphological effect of the polymer substrates on their top ITO layers is observed. Dominant direct and indirect transition types deduced from optical spectra are surprisingly found in ITO films on different polymers. Furthermore, qualitative band structures are figured, and some theoretical discussions about the correlation of optical band structure, interface/surface morphology and carrier density are also presented.

PACS: 73. 20. At, 71. 20. Nr DOI: 10.1088/0256-307X/27/8/087303

Indium tin oxide (ITO) is a heavily doped n-type semiconductor with a high performance in visible transparency and conductivity, so it has been widely utilized as a transparent conducting layer in photoelectric devices.[1−4] The band structure plays a significant role in analyzing semiconductor layers and their contacting properties. Although some theoretical works have been carried out to discuss the band characteristics of crystalline In_2O_3 and/or ITO,[5,6] they would probably encounter some difficulties in practice due to the complex atomic circumstance, conductive mechanism and disorders in real ITO thin films, especially those with low crystalline qualities on polymers. Actually deducing band gap from optical spectra has been proved to be an effective process in practical analysis of ITO thin films.[7−9] Theoretically, in dipole approximation the absorption coefficient α for allowed direct and indirect transitions could be expressed as[10]

$$\alpha h\nu = A(h\nu - E_{\rm opt})^{1/2}, \quad (1)$$

$$\alpha h\nu = B(h\nu - E_{\rm opt} - h\nu_\eta)^2 + C(h\nu - E_{\rm opt} + h\nu_\eta)^2, \quad (2)$$

where $E_{\rm opt}$, $h\nu$ and $h\nu_\eta$ are the optical band gap, photon energy and phonon energy, respectively. A, B and C are constants above zero. Thus, different plots between absorption and photo energy should be observed for different transition types, especially some turning points in indirect transitions.

It is well known that not only the irreproducible interface contacts will influence the devices' performances, but also some surface treatments, which can cause nano-scaled variations of the surface morphology, may significantly affect the devices.[11−13] Such influence has already provided sufficient ground for more attention and further study on the correlations between the surface/interface and the properties of ITO thin films.

In our previous work, the indirect transition band of the ITO films was obtained to effectively expound the electrical and optical properties of those samples.[14] In this work, solid experimental phenomena that indicate some direct and intrinsic interrelation of the surface/interface and the optical band characteristics will be provided. Furthermore, detailed discussions about the different band types and their possible reasons will also be presented.

ITO films were deposited on polymethylmethacrylate (PMMA) and polyethylene terephthalate (PET) by rf-magnetron sputtering at room temperature. The sputtering target used was a 99 mm-diam by 5 mm-thick sintered oxide ceramic disk (90 wt% In_2O_3 and 10 wt%SnO_2, 99.99% purity for both cases). Pure Ar gas (99.9999% purity) was introduced into the vacuum chamber with a base pressure of 5×10^{-5} Pa. The target-substrate distance was 100 mm. ITO thin films with thickness of 140 nm were prepared at sputtering pressure of 1.1 Pa and sputtering powers of 80 W, 120 W and 160 W, respectively.

Surface morphology images, rms surface roughness and the ratio of surface area/projected area (S ratio) were evaluated by atomic force microscopy (AFM). The visible transmittance spectra were measured by a UV-visible spectrophotometer. The carrier density N was analyzed by a Hall Effect measurement system.

Figure 1 shows a morphological effect of the substrate on the top ITO layer. The image of PMMA in Fig. 1(a) shows a very smooth but slightly scraped

*Supported by Program for New Century Excellent Talents in University (NCET-09-0265), Sichuan Provincial Science Foundation for Youths (No 2010JQ0002), State Key Laboratory for Mechanical Behavior of Materials, Xi'an Jiaotong University (No 201011005), and Foundation Franco Chinoise pour la Science et ses Applications (FFCSA), respectively.

**Email: tang@uestc.edu.cn

© 2010 Chinese Physical Society and IOP Publishing Ltd

surface with no grain structure. However, the image of PET in Fig. 1(b) shows a much rougher surface with some dome-shaped grain structure and small cavities and slots. The rms roughness and the S ratio of PMMA are 0.539 nm and 1.004, which are also smaller than those of PET (4.715 nm and 1.021). Consequently, ITO/PMMA samples have homogeneous and smooth surface morphology with small close-packed structures, arrayed regularly with a narrow distribution of size and shape [see Figs. 1(c), 1(e) and 1(g)]. In contrast, many dome-shaped grains of diameters about 50–100 nm are randomly distributed on the surface of ITO/PET [see Figs. 1(d), 1(f) and 1(h)]. Moreover, the rms roughness of ITO/PET (around 10 nm) is much larger than that of ITO/PMMA (below 1nm), and the S ratio of ITO/PET is comparatively greater than that of ITO/PMMA, too. All of these could indicate that ITO/PET has a rougher and larger surface than ITO/PMMA. However, the rms roughness and the S ratio of ITO layers on both PMMA and PET decrease with the increasing sputtering power. The reason might be such that the sputtered atoms or ions with higher kinetic energy at higher sputtering power would more efficiently transfer on the substrate and contribute to the nucleation and better film growth. Some other structural correlations between the top ITO layers and their substrates have also been observed.[15,16]

The transmittance spectra of ITO/PMMA and ITO/PET are presented in Figs. 2(a) and 2(c), respectively. Relationships between absorption and photon energy for ITO/PMMA and ITO/PET films were deduced from the transmittance spectra and plotted in the insets of Figs. 2(a) and 2(c), respectively. According to the figures and Eqs. (1) and (2), dominant allowed direct transitions were found in Fig. 2(a). However, characteristic turning points, which indicate a phonon involved indirect transition, can be found in Fig. 2(c). The indirect transitions in ITO thin films were studied and possible correlations between surface states and transition types were also proposed theoretically.[17–19] This work provides an experimental evidence for this idea.

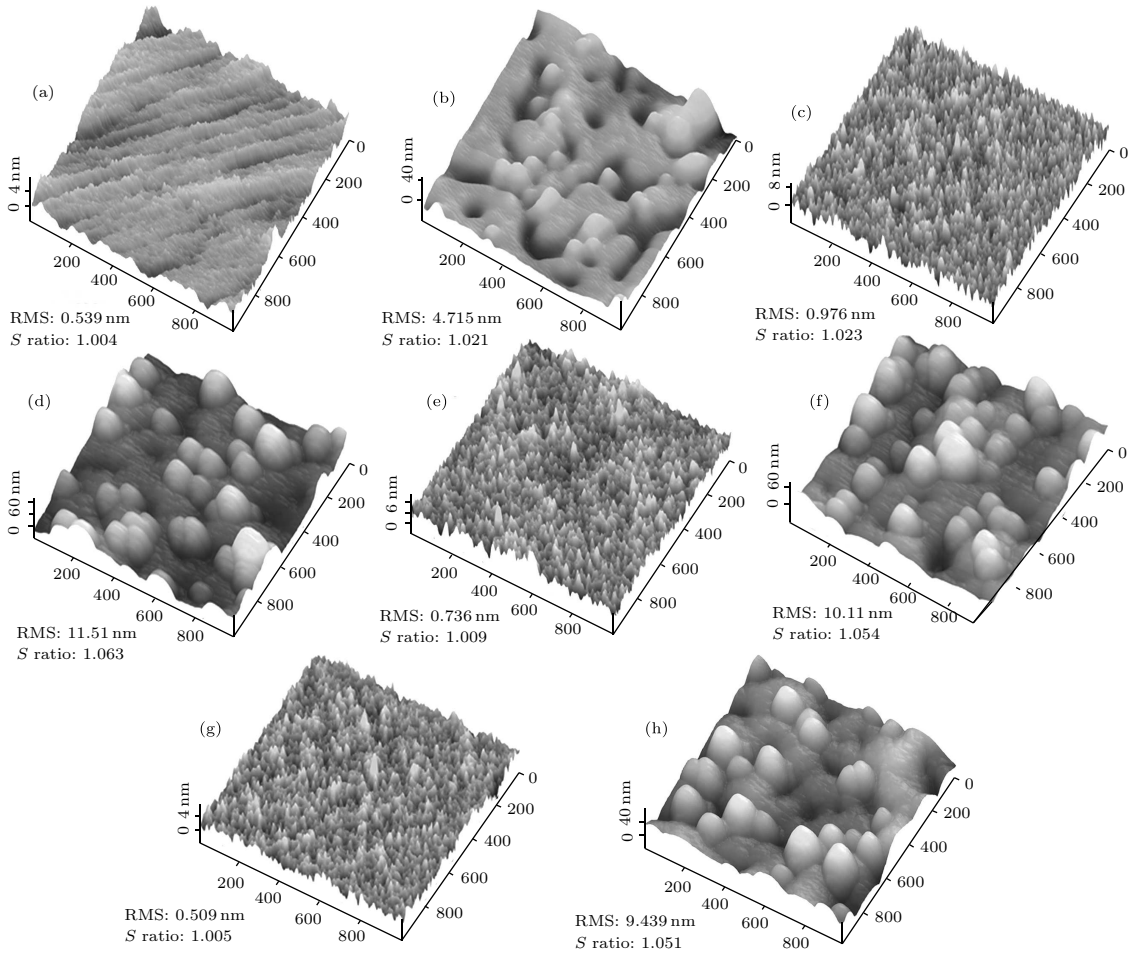

Fig. 1. Three-dimensional AFM images of (a) PMMA, (b) PET and ITO thin films on PMMA and PET at different sputtering powers: (c) ITO/PMMA 80 W, (d) ITO/PET 80 W, (e) ITO/PMMA 120 W, (f) ITO/PET 120 W, (g) ITO/PMMA 160 W and (h) ITO/PET 160 W.

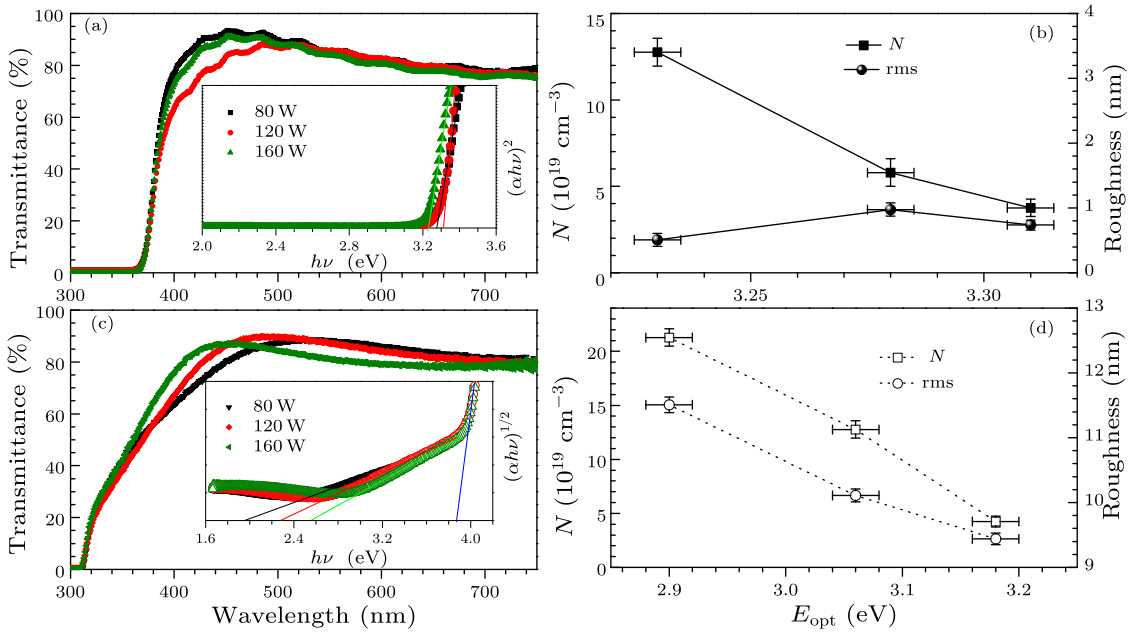

Fig. 2. Visible transmittance spectra of (a) ITO/PMMA and (c) ITO/PET at different sputtering powers. The insets show plots of (a) square and (c) square root of $(\alpha h\nu)$ versus photon energy $h\nu$ for ITO/PMMA and ITO/PET, respectively; and tariations of carrier density N and rms roughtness with respect to optical band gap E_{opt} for (b) ITO/PMMA and (d) ITO/PET.

The optical gap values of ITO/PMMA are 3.28 eV, 3.31 eV and 3.23 eV at sputtering power of 80 W, 120 W and 160 W. Their counterparts of ITO/PET are 2.90 eV, 3.06 eV and 3.18 eV. Moreover, Figs. 2(b) and 2(d) show the variations of carrier density N and rms roughness versus E_{opt} for ITO/PMMA and ITO/PET, respectively. In both ITO/PMMA and ITO/PET the carrier density N decreases with the increasing E_{opt}, which eliminates the possible existence of Burstein–Moss shift[7,8,20] in these samples. Compared to the rapid decrease of E_{opt} in ITO/PET with increasing rms, E_{opt} in ITO/PMMA is not so sensitive to the rms roughness.

Combined with Figs. 1 and 2, the schematic band diagrams emphasizing the band types, the variations of E_{opt} with the sputtering power and the different interface/surface conditions for both ITO/PMMA and ITO/PET are plotted in Fig. 3. Theoretically, the dangling bonds, lattice disorders or other surface/interface related defects in films could serve as the source of surface/interface states.[21] It is possible for the surface/interface states to locate at a point with different K's from the top of valence band. However, the contribution of surface and interface to the properties of many materials can be quite complicated,[22–24] so we should point out that the exact location or shape of the surface states might be different in real materials, which otherwise could lead to similar transitions. The surface/interface states in ITO/PMMA may be not dense enough to affect the direct interband transition shown in Fig. 3(a), so the insensitive and irregular dependence of the E_{opt} on the rms roughness in Fig. 2(b) should be understandable. In contrast, the surface/interface states in ITO/PET may extend deep enough into the band gap, so the indirect transition could more easily occur from the top of valence band to the bottom of the conduction band formed by these surface/interface states [see Fig. 3(b)]. Because of the deeper surface/interface states in the sample with a rougher and larger surface/interface, the decrease of E_{opt} with increasing the rms in Fig. 2(d) should also be reasonable.

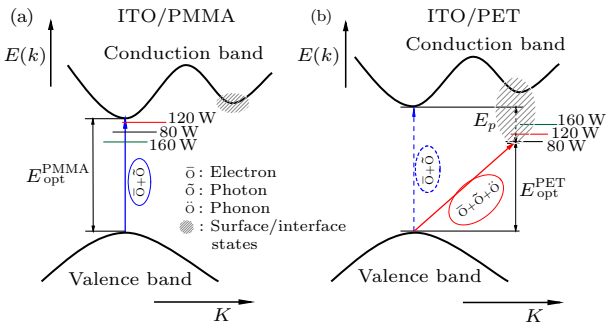

Fig. 3. Schematic band diagrams of (a) ITO/PMMA and (b) ITO/PET.

In addition, the two-step absorptions in the inset of Fig. 2(c) also demonstrate a possible phonon assistant transition process in ITO/PET, because the phonon allows connecting states with the same velocity dE/dk at photon energies greater than those connecting the band-edge excitons.[21] However, if Eq. (2) is quoted to analyze the indirect transition, a process involving electrons, photons and phonons to achieve both energy

and momentum conservations, we will find that the energy $h\nu_\eta$ is too large for a conventional quantum of lattice vibration, i.e. thermal phonons engaged in the momentum conservation. Here, strong electron-phonon interaction[25] might be considered as one mechanism. The phonon, nevertheless, should not be the quantum of lattice vibration any longer, but represent some characteristics of a strong scattering process with the disorders or defects. The energy E_p ($\sim 2h\nu_\eta$) in Fig. 3(b) is still a measure of this interaction strength.[21] Thus, it is reasonable for the film with rougher and larger surface/interface and stronger scattering interaction to have bigger E_p. Therefore, the momentum conservation in the indirect transition of ITO/PET may be satisfied by a strong phonon assistant scattering interaction, which is different from those reported indirect transitions with no phonon assistance.[26–28]

In summary, AFM surface morphologies and visible transmittance spectra of ITO/PMMA and ITO/PET films have been contrastively characterized and studied. Compared to the ITO/PMMA films with direct transitions and smooth interface/surfaces, ITO/PET films are found of indirect transitions and much rougher and lager interface/surfaces. These solid experimental results indicate a possible correlation of the different band types and interface/surface properties. Furthermore, qualitative figures and discussions about the optical band structures, interface/surface morphologies and carrier densities are presented. These properly intrinsic relations of the interface/surface properties and the band structures may provide some ideas and proofs for deliberate layer choice and treatment of photoelectric devices to modify their performances.

References

[1] Krautz D, Cheylan S, Ghosh D S and Pruneri V 2009 *Nanotechnology* **20** 275204
[2] Lee M L, Chi P F and Sheu J K 2009 *Appl. Phys. Lett.* **94** 013512
[3] Wang X R et al 2008 *Chin. Phys. Lett.* **25** 4425
[4] Yu S Y et al 2008 *Chin. Phys. Lett.* **25** 755
[5] Hamberg I and Granqvist C G 1984 *Phys. Rev.* B **30** 3240
[6] Mryasov O N and Freeman A J 2001 *Phys. Rev.* B **64** 233111
[7] Matino F et al 2005 *Phys. Rev.* B **72** 085437
[8] Kim H, Horwitz J S, Kushto G, Piqué A, Kafafi Z H, Gilmore C M and Chrisey D B 2000 *J. Appl. Phys.* **88** 6021
[9] Reddy V S, Das K, Dhar A and Ray S K 2006 *Semicond. Sci. Technol.* **21** 1747
[10] Anselm A I 1981 *Introduction to Semiconductor Theory* (Moscow: MIR Publishers)
[11] Afre R A, Hayashi Y and Soga T 2009 *J. Phys. D: Appl. Phys.* **42** 042002
[12] Kim S H, Jang J and Lee J Y 2006 *Appl. Phys. Lett.* **89** 253501
[13] Kim J S, Park J H, Lee J H, Jo J, Kim D Y and Cho K 2007 *Appl. Phys. Lett.* **91** 112111
[14] Yin X, Tang W, Weng X and Deng L 2009 *J. Phys. D: Appl. Phys.* **42** 025104
[15] Ohta H, Orita M, Hirano M and Hosono H 2002 *J. Appl. Phys.* **91** 3547
[16] Ow-Yang C W, Shigesato Y and Paine D C 2000 *J. Appl. Phys.* **88** 3717
[17] Erhart P et al 2007 *Phys. Rev.* B **75** 153205
[18] Weiher R L and Ley R P 1966 *J. Appl. Phys.* **37** 299
[19] Matino F et al 2005 *Phys. Rev.* B **72** 085437
[20] Burstein E 1954 *Phys. Rev.* **93** 632
[21] Pankove J I 1971 *Optical Processes in Semiconductors* (Englewood Clifts: Prentice-Hall)
[22] Venables J A 2000 *Introduction to Surface and Thin Film Processes* (London: Cambridge University)
[23] García-Moliner F and Flores F 1979 *Introduction to the Theory of Solid Surface* (London: Cambridge University)
[24] Zangwill A 1988 *Physics at Surfaces* (London: Cambridge University)
[25] Street R A 1977 *Solid State Commun.* **24** 363
[26] Pankove J I and Aigrain P 1962 *Phys. Rev.* **126** 956
[27] Hass C 1962 *Phys. Rev.* **125** 1965
[28] Ryvkin S M 1965 *Physica Status Solidi* **11** 285